CHAPTER II

BACKGROUND

2.1 The GOES Satellites

The current NOAA operational geostationary satellites are GOES-8 and GOES-10. The GOES-8 satellite is positioned at 75°W and GOES-10 is located at 135°W. During the normal operational mode, both satellites provide views of North America up to four times an hour and full disk images every three hours. The GOES-8 and GOES-10 satellites are the second and fourth, respectively, of the GOES I-M series. The GOES-11 satellite is currently in orbit ready to replace the next satellite to fail, and GOES-12 was launched in July 2001 and will be ready for operational use by December 2001. Each of the GOES I-M satellites has an expected lifetime of five years. The GOES-8 and GOES-10 satellites have been operational since April 1994 and April 1997, respectively, and therefore GOES-8 is expected to be the next satellite replaced. Further details on the GOES satellites can be found in Menzel and Purdom (1994) and also in the GOES I-M DataBook (Space Systems-Loral 1996; also available online at http://rsd.gsfc.nasa.gov/goes/text/goes.databook.html).

2.1.1 The GOES Satellite Sensors

There are two earth-sensing instruments, the Imager and the Sounder, on board each GOES satellite. The Imager sensor has five channels, one in the visible range of the electromagnetic spectrum, and four within the IR region (Table 2.1). The Imager visible channel has 1 km resolution at nadir (with a sampled subpoint resolution of 0.57 km in the east-west direction by 1.0 km in the north-south direction), the IR channels 2, 4, and 5 have nadir resolution of 4 km (with a sampled subpoint resolution of 2.3 km by 4.0 km), and the water vapor channel 3 has 8 km resolution (with a sampled subpoint resolution of 2.3 km by 8.0 km). The Sounder has 18 IR channels plus one visible channel (Table 2.2). All of the Sounder channels have 8 km resolution at nadir but sample every 10 km; therefore, the Sounder nominal resolution is described as 10 km. The Sounder IR channels are divided into the longwave group (channels 1-7), the midwave group (channels 8-12), and the shortwave group (channels 13-18).

Each of the Imager channels has a separate set of detectors positioned in a north-south array that scan in east-west and west-east directions on alternate lines Dorsey et al. 1988). The Imager visible channel has eight detectors, channels 2, 4, and 5 each have two detectors, and channel 3 has one. The Sounder has four separate detector arrays, with the visible channel using one set of four detectors and the IR channels using three sets of four detectors. Each set of IR detectors on the Sounder samples one of the three groups of IR channels. The Sounder also scans in east-west and west-east directions.

The Imager and Sounder instruments have different scanning schedules and domains (Figures 2.1 and 2.2 respectively). Figure 2.1 shows the different sectors scanned by the Imager in its routine scanning mode. The Sounder is operationally

Table 2.1 GOES-8 Imager characteristics.

Channel number	Channel wavelength (μm)	Description	Spatial Resolution (km)	Number of detectors
1	0.52 - 0.72	Visible	1	8
2	3.78 - 4.03	Shortwave IR window	4	2
3	6.47 - 7.02	Upper-level water vapor	8	1
4	10.2 - 11.2	Longwave IR window	4	2
5	11.5 - 12.5	Longwave IR window	4	2

Table 2.2 GOES-8 Sounder characteristics.

Channel number	Central wavelength (μm)	Detector	Purpose
1	14.71	longwave	Stratospheric temp
2	14.37		Tropopause temp
3	14.06		Upper-level temp
4	13.64		Midlevel temp
5	13.37		Low-level temp
6	12.66		Total PW
7	12.06		ST, moisture
8	11.06	midwave	ST
9	9.71		Total ozone
10	7.43		Low-level moisture
11	7.02		Midlevel moisture
12	6.51		Upper-level moisture
13	4.57	shortwave	Low-level temp
14	4.52		Midlevel temp
15	4.45		Upper-level temp
16	4.13		Boundary-layer temp
17	3.98		ST
18	3.74		ST, moisture
19	0.67	visible	Cloud detection

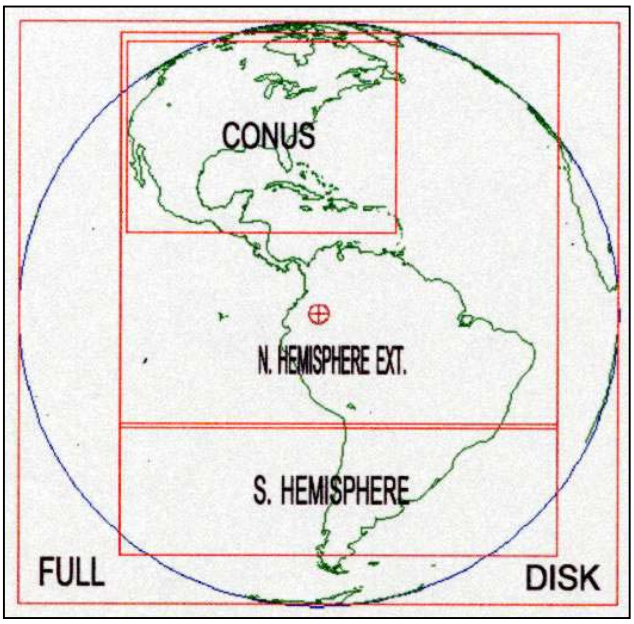

Figure 2.1 GOES-East Imager routine scanning sectors (Satellite Services Division (SSD)/NOAA 2001).

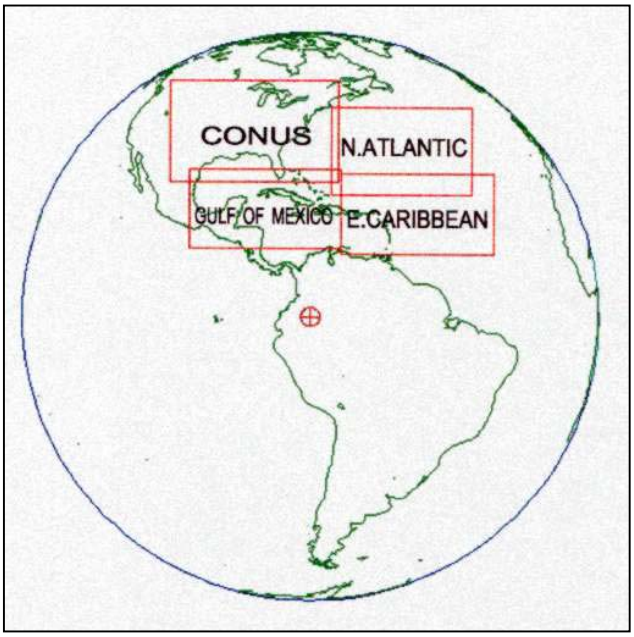

Figure 2.2 GOES-East Sounder routine scanning sectors (SSD/NOAA 2001).

scheduled to provide images of only the northern hemisphere, as shown in Figure 2.2. The Sounder scanning sectors are both spatially and temporally limited because of the longer time required for the Sounder to scan a scene because of its many channels. The Sounder produces two images per hour, one of the CONUS and the other over an ocean region. The smaller sectors and less frequent imaging of the Sounder are drawbacks of using the Sounder instead of the Imager.

2.1.2 The GOES Imager and Sounder Spectral Bands

As mentioned previously, the Imager has five spectral bands and the Sounder has 19 spectral bands. The five Imager channels have the following wavelength intervals: 0.52-0.72 μm (visible), 3.78-4.03 μm (shortwave IR), 6.47-7.02 μm (water vapor), 10.2-11.2 μm and 11.5-12.5 μm (longwave IR window) (Menzel and Purdom 1994). The Sounder central wavelengths of the 19 channels range from 0.67 μm (visible channel 19) to 14.71 μm (longwave channel 1). The Sounder channels of interest for this research are the three channels, 6, 7, and 8, within the longwave IR window (Table 2.2). The center wavelengths for bands 6, 7, and 8 are 12.66 μm, 12.06 μm, and 11.03 μm, respectively. The bands of interest for this research are those located in the 10-13 μm longwave IR atmospheric window because the retrieval technique utilizes information from channels within this region. The Imager has two bands (4 and 5) and the Sounder has three bands (6, 7, and 8) within the longwave IR window. Upwelling radiation from the surface in the 10-13 μm atmospheric window is partially absorbed by water vapor in the atmosphere. By using at least two channels within the same window, the effects of the atmospheric water vapor absorption can be eliminated in the retrieval process.

Figure 2.3 shows the spectral response curves of the GOES-8 Imager and Sounder IR window channels, and the atmospheric transmittance observed by the satellite for a typical atmospheric temperature and moisture profile. The spectral response functions describe the wavelength range of each band and the sensitivity of the entire optical system (e.g., detector, optics) to the radiation within the wavelength range. The total column atmospheric transmittance plot in Figure 2.3 describes the portion of radiation emitted from the surface reaching the top of the atmosphere as a function of wavelength. For the 11 μm window channels of the Imager and Sounder, the atmospheric transmittance is relatively large, and thus a significant portion of the radiation signal received by the satellite is from the surface. For the 12 μm channels, additional water vapor absorption reduces the atmospheric transmittance. For this reason, the 12 μm channels are sometimes referred to as "dirty" channels. To correct for the atmospheric absorption of the upwelling radiation and obtain the true emission from the surface, two channels within the same window are used. By utilizing two channels with similar wavelengths, the difference between the two channels is assumed to be the result of the differential absorption of water vapor in the atmosphere. Thus, the atmospheric absorption component can be removed and the surface temperature determined. The Imager will become obsolete with respect to this split-window retrieval approach starting with the GOES-12 satellite because of the loss of the 12 μm channel.

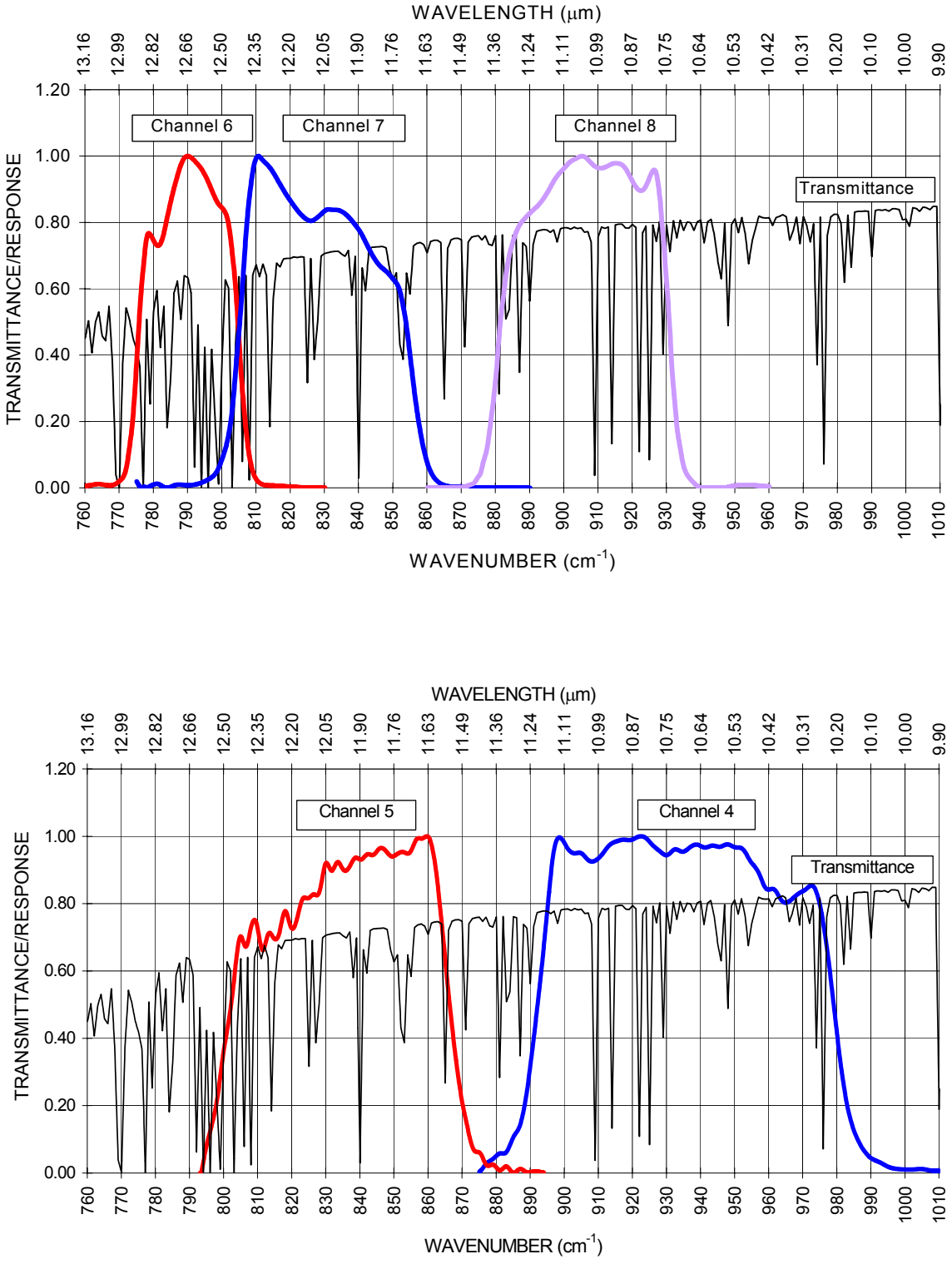

Figure 2.3 GOES-8 spectral response curves and atmospheric transmittance in the infrared window region for the Sounder (top panel) and the Imager (bottom panel).

2.1.3 Calibration of the GOES Sensors

The GOES satellites collect raw Imager data (10 bit words) and raw Sounder data (13 bit words). The raw data are transmitted to the Command and Data Acquisition Station (CDA) at Wallops, Virginia. The data are processed, sent back to the satellite, and then retransmitted in GOES VARiable (GVAR) data format to users. Data for calibration of the IR channels is acquired on-board, to help determine the absolute radiometric temperature of the scene viewed by the sensors. The noise in the calibration equations causes both random noise in the radiances and systematic striping within images. The calibration data is filtered and averaged to reduce the noise. The raw data in the visible images are not calibrated but are normalized at the CDA (Weinreb et al. 1997). The following sections explain the on-board collection of calibration data, the occurrence of striping, and the conversion of raw IR data to GVAR format and then to radiances and temperatures. Visible data calibration, noise, and conversion are not discussed because of the irrelevance to this research.

2.1.3.1 Infrared On-Board Calibration Data

Temperatures on the GOES satellite sensors vary diurnally by tens of degrees Kelvin. These large and fast temperature changes cause the instruments' IR responsivities to vary significantly (Weinreb et al. 1997). The IR channels of the Imager and Sounder are calibrated frequently to counteract these temperature changes. To calibrate their IR channels, the Imager and Sounder view space and warm on-board blackbodies of known temperatures. The data from blackbody looks are used to develop the slopes of the calibration equations. The data from space looks determine the

calibration intercepts. The Sounder views space every 2 minutes and its blackbody every 20 minutes. The Imager needs to view space as often as possible to reduce the effect of 1/f noise. For routine imaging, the Imager views space every 36.6 seconds, and during a full disk image the space look interval is 2.2 seconds. The Imager views its blackbody every 30 minutes.

2.1.3.2 Random Noise and Striping in Calibrated Infrared Images

Some amount of the noise remains after smoothing of the calibration equations, and causes random errors in the radiances and systematic striping in the images (Weinreb et al. 1997). The random noise component results from the measurement uncertainty of the instrument. The image striping results from the systematic error of each detector that is caused by inconsistencies in their calibration slopes. The GOES satellites exhibit striping in both Imager and Sounder calibrated IR images. Stripes are seen in the east-west direction as a result of multiple detectors scanning the scene. Striping occurs on uniform scenes as a result of the differences in output of the detectors in a channel (Baucom and Weinreb 1996). Baucom and Weinreb (1996) state that for GOES-8 Imager channels 4 or 5 striping magnitudes of several tenths of a Kelvin are common within 290 K scenes. The main cause of striping in Imager scenes is low frequency, or 1/f, noise in the calibration of the detectors (Wack and Candell 1996). The 1/f noise causes a random drift of the output of each detector during calibration and imaging and therefore the noise exhibited in each detector is unrelated (Baucom and Weinreb 1996).

The Sounder does not suffer from 1/f-noise drifts since the Sounder performs clamps while viewing its filter wheel at a frequency of 50Hz (Weinreb et al. 1997). The

complete explanation for the striping seen in Sounder calibrated images is unknown. It is believed that the main cause for the Sounder striping is the different responses of the four detectors to the changes in background flux caused by the changes of on-board temperatures (Weinreb, M. personal communication 2001). Also, the relatively long time between space looks (2 minutes) amplifies the problem.

Random noise and striping within GOES-11 calibrated images is of interest to this research because of the possibility of GOES-11 replacing GOES-8. During the GOES-11 science test performed during the summer of 2000, the GOES-11 Sounder was seen to exhibit both less noise and less striping than GOES-8 (Daniels and Schmit 2001). Figure 2.4 compares random noise levels from the Sounders from GOES-8 and GOES-11 to specifications and shows improvement in noise levels in GOES-11 over GOES-8 for the shortwave and longwave regions of the IR. The circled region in Figure 2.4 highlights the longwave IR window channels 6, 7, and 8. The GOES-11 channels 6 and 7 both exhibit reductions in noise compared to GOES-8. The GOES-11 channel 8 shows a slight increase in noise compared to GOES-8 channel 8, but still below the specification level for that channel. The noise levels for the three split window channels all fall in the 0.1 – 0.2 $mW/m^2/ster/cm^{-1}$ range, resulting in approximately 0.1 K noise in the brightness temperatures.

2.1.3.3 Conversion of Infrared Data in GVAR format

The raw Imager and Sounder data are transmitted to the CDA in Virginia in 10-bit words and 13-bit words, respectively. Calibration coefficients determined from on-board calibration are applied to the raw IR data at the CDA in real time, converting the raw data

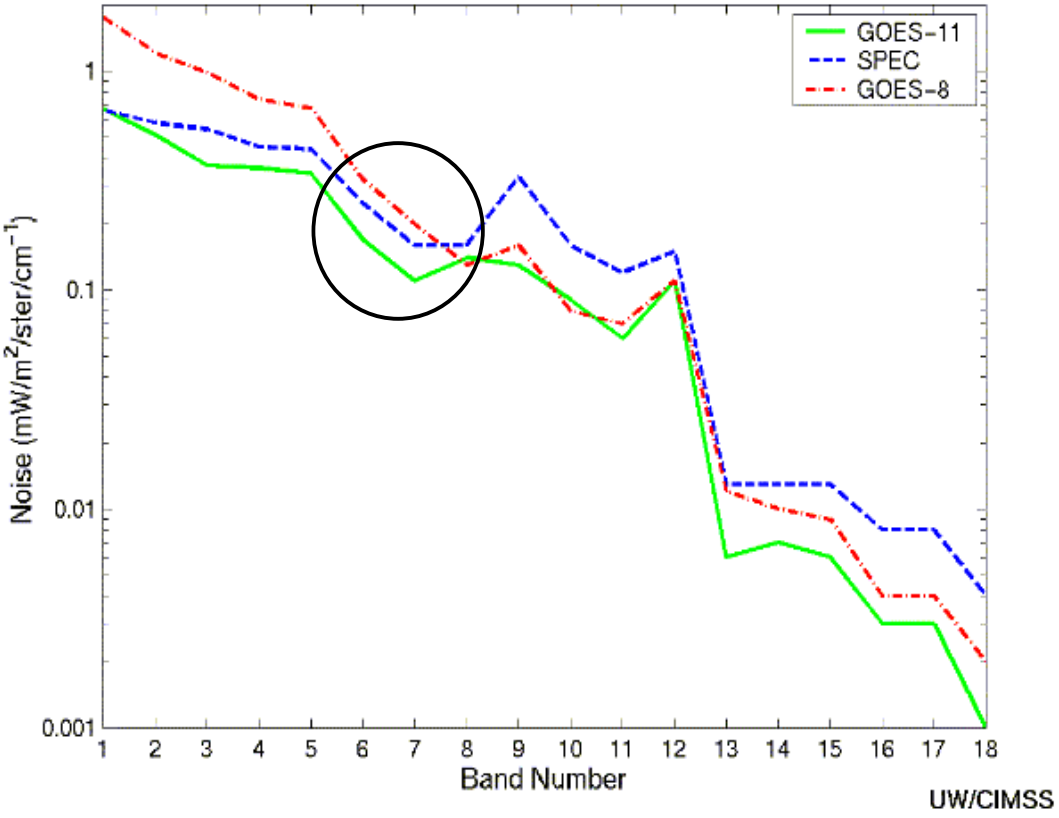

Figure 2.4 Comparisons of GOES-8 and GOES-11 space noise levels to specifications (Daniels and Schmit 2001).

to radiances. The radiances are scaled to exploit the full word length of the GVAR, 10-bit words (0-1023) for Imager data or 16-bit words (0-65535) for the Sounder data (Weinreb et al. 1997). The processed data in GVAR format is then transmitted back to the satellite and then retransmitted to the users. The following description of conversion of GVAR counts to radiances and temperatures is adapted from Weinreb et al. (1997).

The GVAR counts are easily converted to radiances by the user using the following equation,

$$R = \left(X_G - B\right)/M \,, \tag{2.1}$$

where R is radiance in mW/(m^2-sr-cm^{-1}), X_G is the GVAR count, B is the scaling intercept, and M is the scaling slope. The scaling intercept and slope values are dependent on the channel but not the detector and are expected to remain constant. GOES-8 Imager scaling coefficients can be found in Weinreb et al. (1997). The GOES-8 Sounder scaling coefficients are found in an updated version of Weinreb et al. (1997) available online at http://www.nnic.noaa.gov/SOCC/page1.htm.

The radiance values are converted to effective temperatures using the inverse Planck function, Equation (2.2),

$$T_{eff} = \frac{\left(c_2 \upsilon\right)}{\ln\left(1 + \frac{c_1 \upsilon^3}{R}\right)} \,, \tag{2.2}$$

where υ is the central wavenumber of the channel, T_{eff} is the effective temperature in

Kelvin, and c_1 and c_2 are radiation constants given by,

$c_1 = 1.191066 \times 10^{-5}$ mW/(m^2-sr-cm^{-4})

$c_2 = 1.438833$ K/cm^{-1}.

The effective temperature accounts for the variation of the Planck function across the spectral band of the channel. The actual temperature T (K) can be derived from the effective temperature and constants α and β (available online at http://www.nnic.noaa.gov/SOCC/page1.htm), which vary with instrument, channel and detector, using Equation (2.3):

$$T = \beta\ T_{eff} + \alpha. \tag{2.3}$$

2.2 Physical Split Window Retrieval Technique

The satellite retrieval technique used for this research is the Physical Split Window (PSW) technique developed by Jedlovec (1987) originally intended for use with aircraft data. The PSW algorithm is similar to the technique described by Hayden et al. (1996) used to produce derived product imagery from GOES. The PSW technique uses channels 4 and 5 of the Imager or two of the three channels 6, 7 and 8 of the Sounder, to simultaneously retrieve skin temperature and total precipitable water (Suggs et al. 1998). The method solves for perturbations of ST and PW from initial guess values. Required *a priori* information includes vertical profiles of temperature and moisture, total PW and ST. The initial guess values of temperature and moisture are obtained from radiosondes or numerical models. For the retrievals generated in this research, the first-guess profiles,

ST, and PW are obtained from the 00 UTC cycle forecast of the MM5 model run operationally at the GHCC (Lapenta et al. 1999). The forecasted surface air temperature is used as the first-guess ST in the retrieval process.

The PSW technique is derived from a perturbation form of the radiative transfer equation. The technique determines the bulk layer parameter PW and surface ST, not vertical profiles. The following description of the PSW algorithm is adapted from Suggs et al. (1998). The perturbations of skin temperature δT_s and total precipitable water δU_{ps} from the first-guess values are retrieved using the perturbation Equation (2.4), with emissivity assumed to be one,

$$\delta I - \varepsilon_I = C\delta T_s + (D - \varepsilon_D)\delta U_{ps}, \tag{2.4}$$

where δI is the difference in the radiance between that observed by the satellite and that calculated using the first-guess temperature and moisture profiles. C and D are coefficients sensitive to the guess temperature and moisture profiles and the surface skin temperature, and are given by

$$C = \bar{\tau}_{ps} \frac{\partial B(\bar{T}_s)}{\partial T},$$

$$D = \frac{\partial \bar{\tau}_{ps}}{\partial U}\left[B(\bar{T}_s) - B(\bar{T}_{ps})\right] - \frac{1}{\bar{U}_{ps}} \int_{ps}^{0} \bar{U}(p) \frac{\partial \bar{\tau}(p)}{\partial U} \frac{\partial B\left[\bar{T}(p)\right]}{\partial p} dp, \tag{2.5}$$

where the subcript s refers to the surface, the subscript ps denotes that the atmospheric parameter is evaluated at the surface pressure, and the overbar denotes a first-guess value.

The quantities τ, B, T and p are the atmospheric transmittance, the Planck function, temperature, and pressure, respectively. The quantities ε_I and ε_D are residuals and are assumed small compared to δI and the coefficient D, respectively, and are therefore set to zero.

Suggs et al. (1998) provides a full derivation of the perturbation equation. The derivation begins with Equation (2.6), the radiative transfer equation for upward radiation assuming an emissivity of one and a nonscattering, plane-parallel atmosphere

$$I = B\lambda(T_S)\tau_{ps} + \int_{ps}^{0} B\lambda(T_P)\frac{\partial\tau(p)}{\partial p}dp\,, \tag{2.6}$$

where $\tau = e^{-t}$ and t is the absorption optical thickness which describes the ability of the atmosphere to absorb radiation within the wavelength interval associated with the sensor IR window channel. The two unknowns (δT_s and δU_{ps}) in the perturbation Equation (2.4) can be retrieved simultaneously using two different IR window channels to create two separate equations. The least squares solution for ST is found using

$$\delta T_s = \frac{\delta I_{\lambda 1} D_{\lambda 2} - \delta I_{\lambda 2} D_{\lambda 1}}{C_{\lambda 1} D_{\lambda 2} - C_{\lambda 2} D_{\lambda 1}} \tag{2.7}$$

with the retrieved skin temperature values represented as

$$T_s = \overline{T}_s + \delta T_s\,. \tag{2.8}$$

The subscripts $\lambda 1$ and $\lambda 2$ refer to the two channels of data. The final skin temperature value is T_s, where $\overline{T_s}$ is the guess skin temperature and δT_s is the retrieved perturbation of skin temperature arrived at from the satellite observations.

The PSW algorithm contains a number of assumptions which can effect the accuracy of the technique. The main assumptions are that the surface emissivity is 0.98, the emission is isotropic, the first guess profiles are close to observed profiles, and that the surface air temperature is a good approximation for the guess skin temperature. The constant emissivity assumption can be a significant source of error in the retrievals. A 2% change in emissivity can result in approximately 1 K (depending on a number of factors including the surface temperature and the atmospheric transmittance) change in brightness temperature. Suggs et al. (1998) discussed these assumptions and the accuracy of the algorithm and found algorithm retrieval bias errors (assuming no error resulting from the emissivity assumption or from noise errors) of ST ranging from –0.3 to 0.1 K and standard deviation errors of 0.1 to 0.9 K for the GOES-8 Imager and Sounder for varying first-guess times. The largest errors were produced from retrievals with times furthest away from the time of the first-guess field, and when the combinations of Sounder channels 6 and 8 (as opposed to using channels 7 and 8) were used. Additional evaluations of the retrieval accuracy of the PSW algorithm on real data have been presented by Knabb and Fuelberg (1997) and Suggs et al. (2001). Comparisons between three PW retrieval algorithms (Knabb and Fuelberg 1997) found that the PSW technique performed well, with smaller bias and standard deviation values than the other two methods.

2.3 Cloud Masking Technique

When making surface retrievals using satellite data, it is essential to avoid cloudy pixels and to make retrievals for all the possible clear pixels. Clouds contaminate surface retrievals made using satellite data; therefore, to avoid cloud contamination, a cloud mask is produced. The IR window channels of the sensors on the GOES satellites measure the radiance emitted from either the land or sea surface or from cloud tops. For thin clouds, both the surface and the cloud contribute to the measured radiance. If a pixel is cloudy or partly cloudy but surface retrievals are derived from the pixel, the retrieved ST value will not be a true representation of the surface temperature for that pixel. To avoid contaminated surface retrievals, cloudy pixels need to be recognized and removed from the retrieval process. Detecting clouds in one particular image is a relatively simple task, but to develop an approach to work well at all times of the day throughout the year has proven to be difficult.

A cloud mask labels pixels as either clear or cloudy. The GHCC cloud mask algorithm uses a bi-spectral spatial coherence approach, which was developed for use with the GOES Imager (Guillory et al. 1998). The same algorithm is applied to the GOES Sounder without adjustment. The algorithm is applied to a difference image, the Imager 10.7 μm minus 3.9 μm channel difference, or the Sounder 11.03 μm minus 3.74 μm channel difference. The 3.9 μm (or 3.74 μm) shortwave IR channel has both an emissive and a reflected IR component. The difference between the longwave IR channel and the shortwave IR channel is much larger over clouds than over the surface during the daytime. This is because the difference between the 11 μm and 3.9 μm emissivities is much larger over clouds than over the land or sea surface. The smaller

emissivity values at 3.9 μm over clouds allow a larger portion of the incident solar radiation to be reflected back to the satellite sensor thus causing higher radiances to be measured. The bi-spectral spatial coherence technique utilizes two spatial tests and one spectral threshold method, all applied to the 11 μm – 3.9 μm difference image. First, a standard deviation threshold (2.8 K) is used to detect cloud edges. Second, a difference threshold (2.1 K) between adjacent pixels is used to fill in around the cloud edges. Third, an IR temperature difference threshold (11.5 K) test is applied as a final check. More information on this cloud mask technique and details concerning operational use can be found in Guillory et al. (1998) and Jedlovec and Laws (2001).

The technique works relatively well during midday times, but has trouble detecting clouds during periods with low sun angles, i.e., early morning and late evening, because the difference between the two channels becomes small for both cloudy and clear scenes. There are significant differences between the Imager and Sounder cloud masks because the two instruments have differences in their spectral bands and spatial resolutions. Figure 2.5 presents an example of the Imager (top right panel) and the Sounder (top left panel) cloud masks and the corresponding visible (bottom left panel) and IR (bottom right panel) images for 1345 UTC April 25, 2001. The circles indicate regions where the Imager under determines the presence of clouds or where the Sounder over determines clouds. The Sounder cloud mask is more cloud-conservative than the Imager cloud mask for all times of the day and throughout the year. Because of the importance of avoiding cloud-contaminated pixels, the Sounder cloud mask is normally a better representation of the cloud cover. Work is currently being performed at the GHCC to improve our cloud masking technique (Jedlovec and Laws 2001).

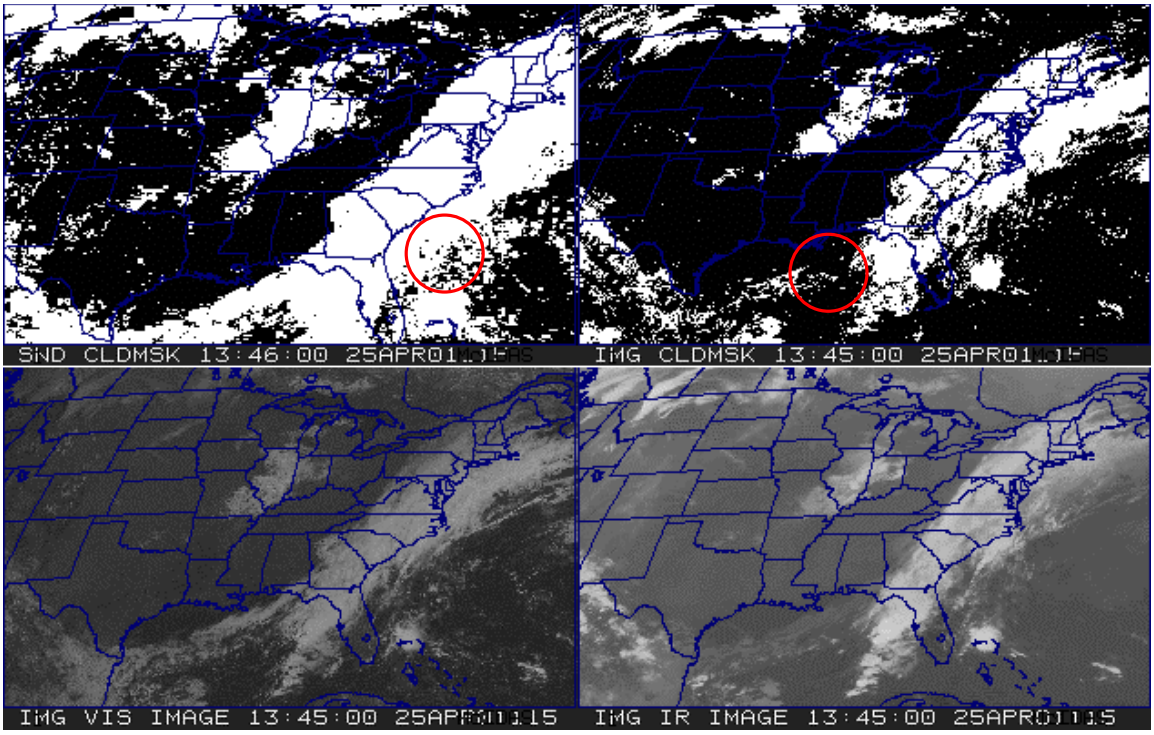

Figure 2.5 Sounder (top left) and Imager (top right) cloud masks, and the Imager visible (bottom left) and infrared (bottom right) images at 1345 UTC on April 25, 2001.